Since January 2020 Elsevier has created a COVID-19 resource centre with free information in English and Mandarin on the novel coronavirus COVID-19. The COVID-19 resource centre is hosted on Elsevier Connect, the company's public news and information website.

Virology 390 (2009) 356–367

Contents lists available at ScienceDirect

Virology

journal homepage: www.elsevier.com/locate/yviro

Analyses of the spleen proteome of chickens infected with Marek's disease virus

Niroshan Thanthrige-Don [a], Mohamed F. Abdul-Careem [a], L. Allen Shack [b], Shane C. Burgess [b,1], Shayan Sharif [a,*,1]

[a] Department of Pathobiology, Ontario Veterinary College, University of Guelph, Guelph, Ontario, Canada N1G 2W1
[b] Department of Basic Sciences, Mississippi State University, USA

ARTICLE INFO

Article history:
Received 13 April 2009
Returned to author for revision 29 April 2009
Accepted 18 May 2009
Available online 21 June 2009

Keywords:
Marek's disease virus
Host response
Chicken proteome
2D gel electrophoresis
1D LC ESI MS/MS

ABSTRACT

Marek's disease virus (MDV), which causes a lymphoproliferative disease in chickens, is known to induce host responses leading to protection against disease in a manner dependent on genetic background of chickens and virulence of the virus. In the present study, changes in the spleen proteome at 7, 14 and 21 days post-infection in response to MDV infection were studied using two-dimensional polyacrylamide gel electrophoresis. Differentially expressed proteins were identified using one-dimensional liquid chromatography electrospray ionization tandem mass spectrometry (1D LC ESI MS/MS). Comparative analysis of multiple gels revealed that the majority of changes had occurred at early stages of the disease. In total, 61 protein spots representing 48 host proteins were detected as either quantitatively (false discovery rate (FDR) $\leq$0.05 and fold change $\geq$2) or qualitatively differentially expressed at least once during different sampling points. Overall, the proteins identified in the present study are involved in a variety of cellular processes such as the antigen processing and presentation, ubiquitin–proteasome protein degradation (UPP), formation of the cytoskeleton, cellular metabolism, signal transduction and regulation of translation. Notably, early stages of the disease were characterized by changes in the UPP, and antigen presentation. Furthermore, changes indicative of active cell proliferation as well as apoptosis together with significant changes in cytoskeletal components that were observed throughout the experimental period suggested the complexity of the pathogenesis. The present findings provide a basis for further studies aimed at elucidation of the role of these proteins in MDV interactions with its host.

Introduction

Marek's disease (MD) in chickens is caused by Gallid herpesvirus 2 (GaHV-2) or Marek's disease virus (MDV). Hereafter, this virus is referred to as MDV. MDV is a highly prevalent alpha-herpesvirus and the disease it causes is characterized by transient neurological signs and immunosuppression at early stages that could subsequently be followed by lymphoma formation in various visceral organs in susceptible birds. Upon infection via inhalation, in all infected birds, MDV is taken to various lymphoid organs, such as spleen, thymus and bursa of Fabricius where early cytolytic infection in B cells that proceeds to latent infection of T cells occurs. While a lifelong latent phase could occur in genetically MD-resistant birds and in those protected by vaccination, late reactivation of latent virus in susceptible birds could cause transformation of mainly CD4+ T cells, leading to lymphoma formation. Meanwhile, active replication of MDV occurs in feather follicles of infected birds regardless of their genetic susceptibility rendering them a continuous source of infectious viruses (Baigent and Davison, 2004). Although MD is currently controlled by vaccination, there have been periodical MD outbreaks caused by new strains of MDV with increased virulence (Witter, 1997). The potential of MDV to evolve and overcome vaccinal immunity is considered as a major threat for a sustainable MD control strategy. However, many aspects of MDV–host interactions are still being elucidated (Baaten et al., 2004).

To date, several studies have been conducted to examine host gene expression in response to MDV infection on a relatively large scale using various genomic techniques, such as microarrays. Changes in gene expression of chicken embryo fibroblasts (CEF) infected with RB1B, a very virulent strain of MDV, were studied by Morgan et al. (2001) using a microarray containing 1126 expressed sequence tags. These authors reported the differential expression of a number of host genes including those associated with inflammation, antigen presentation and cell growth. An *in vivo* study by our group using the same virus strain and a small-scale microarray has revealed significant changes in the expression of genes encoding cell surface molecules, transcription and signal transduction molecules as well as cytokines (Sarson et al., 2006). While studies of this nature, in the context of MD in particular and various other viruses in general (reviewed in Piersanti et al., 2004) would certainly enhance our understanding of host–pathogen interactions, further expansion of this knowledge with

* Corresponding author. Fax: +1 519 824 5930.
E-mail address: shayan@uoguelph.ca (S. Sharif).
[1] This work is a joint collaboration between these principal investigators.

0042-6822/$ – see front matter © 2009 Elsevier Inc. All rights reserved.
doi:10.1016/j.virol.2009.05.020

proteomic studies is still important (reviewed in Burgess, 2004; Zhang et al., 2005). This is partly because of the possible inconsistency between the expression of genes at the transcript and protein levels (Gygi et al., 1999). Furthermore, viruses can induce post-translational modifications in host proteins without affecting the mRNA expression (Liu et al., 2001).

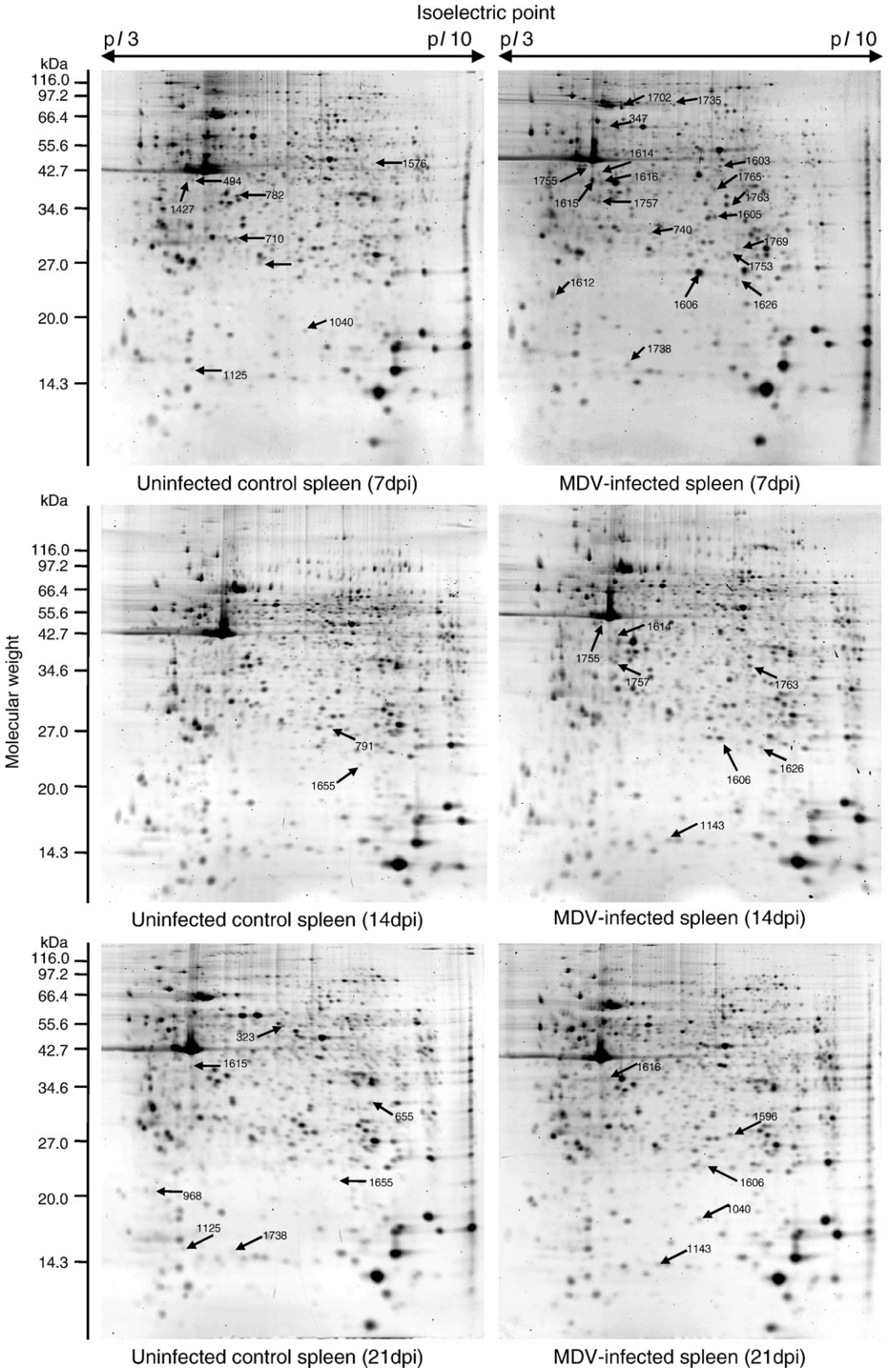

Fig. 1. Representative 2D gel images of MDV-infected and uninfected control spleen proteomes with their respective sampling points. Arrows with accompanying spot numbers show successfully identified protein spots that were uniquely expressed (qualitative differences) in each group at corresponding time point. Please refer to Table 1 for identities of corresponding spot numbers and to Fig. 2 for the map of quantitatively differentially expressed spots.

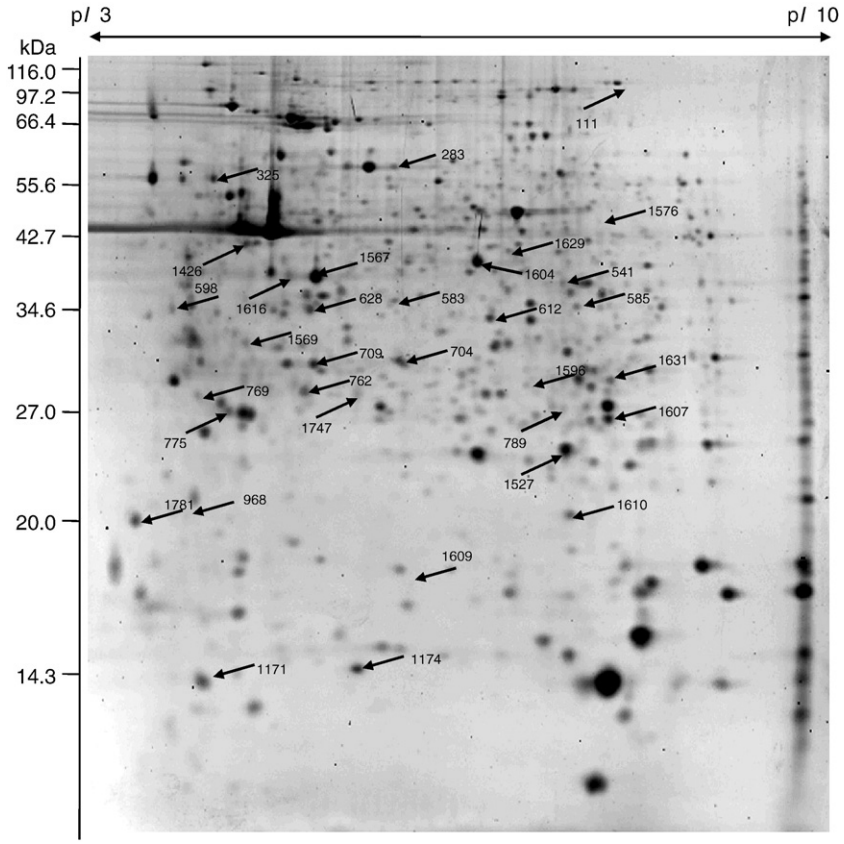

Fig. 2. A representative gel image showing 2D gel electrophoresis map of the relative locations of spots that displayed significant quantitative differential expression (FDR ≤ 0.05 and fold change ≥ 2) at least once during different sampling times. This image represents the proteome of 7 dpi MDV-infected spleen. Because of the absence of certain spots in this gel, arrows for spot 111, 968, 1576 and 1609 represent the relative positions only. Please refer to Table 1 for identities of corresponding spot numbers and to Fig. 1 for maps of qualitatively differentially expressed spots.

In a recent *in vitro* proteomic study, Ramaroson et al. (2008) inventoried 1460 and 1676 proteins expressed in MDV-infected and mock-infected CEF, respectively. Several other proteomic studies in the context of MD have been conducted to model the proteome of MDV-transformed CD4+ T lymphocytes *in vitro*. Notably, proteomic modeling of MDV-transformed CD30^{hi} CD4+ T lymphocytes has suggested that these cells exhibit a regulatory T cell phenotype (Buza and Burgess, 2007; Shack et al., 2008). Further, such studies have been able to describe the fundamental differences between MDV-transformed T cells and their non-transformed healthy counterparts with regard to activated signalling pathways (Buza and Burgess, 2008). With respect to viral protein expression, Liu et al. (2006) identified a number of unique proteins expressed during the lytic phase of MDV-infected CEF using a mass spectrometry-based proteomic approach. These studies highlight the potential of various proteomic tools in understanding the dynamics of host–pathogen interactions during various phases of MD.

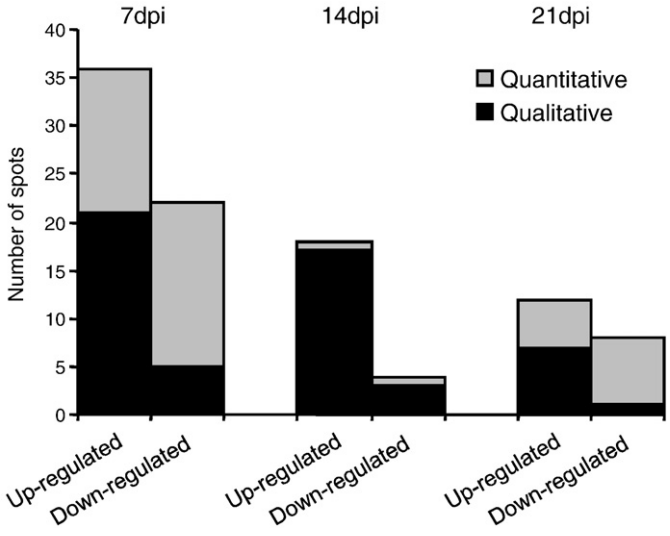

Fig. 3. Comparison of total numbers of significantly differentially expressed protein spots in MDV-infected spleens at various sampling time points. In calculation of total number of spots in each category, newly induced protein spots were considered as up-regulation and the absence of spots compared to uninfected controls was considered as down-regulation.

The current study was intended to investigate the dynamics of host protein expression across the various phases of MDV life cycle in MDV-infected chickens. While we were able to detect more than 500 separate protein spots for each sample, here we report more than 60 significantly differentially expressed proteins identified using two-dimensional gel electrophoresis (2DE) and mass spectrometry. Putative importance of some of these proteins in the context of MD is discussed.

Results

Spot profiles of 2D PAGE of MDV-infected and uninfected control chicken spleens

Proteins from spleens of MDV-infected and uninfected control chickens at 7, 14 and 21 days post-infection (dpi) were extracted and analyzed by 2DE in order to compare the protein expression profiles between each group. On average, 517 ± 84 distinct protein spots could be resolved by 2DE using pH 3-10NL IPG strips loaded with

Table 1
List of differentially expressed protein spots in MDV-infected spleen tissues identified by 1D LC ESI MS/MS.

Ref. spot no.	Protein name[a]	Fold change in expression			Number of peptides identified	Protein coverage[b] (%)	Probability	Protein score[c]	Accession no.	Mr. (predicted/observed) (kDa)
		7 dpi	14 dpi	21 dpi						
Cellular structural proteins										
1738	PREDICTED: similar to Coactosin-like 1 (*Dictyostelium*) (COTL1)	IN	1.6	REP	1	17	5.3E−12	5.62	gi|118096533	15.9/15.34
628	Beta-actin (ACTB)	4.2	1	1.1	3	12	5.0E−40	28.36	gi|45382927	41.7/34.23
1614	Beta-actin (ACTB)	IN	IN	AB	1	3	0.00028	2.95	gi|45382927	41.7/37.84
1616	Beta-actin (ACTB)	IN	4.9	IN	4	28	7.8E−69	38.18	gi|45382927	41.7/36.15
1757	Beta-actin (ACTB)	IN	IN	AB	2	9	1.2E−28	16.17	gi|45382927	41.7/34.20
1567	Beta-actin (ACTB)	2.5	2	1.8	4	19	6.2E−55	41.75	gi|45382927	41.7/36.54
1615	Actin, alpha 2, smooth muscle, aorta (ACTA2)	IN	AB	REP	2	8	1.4E−12	5.93	gi|71895043	42.0/36.90
762	Actin, alpha 2, smooth muscle, aorta (ACTA2)	4.2	1.8	1.3	4	11	1.8E−38	26.37	gi|71895043	42.0/28.52
709	Actin, alpha 2, smooth muscle, aorta (ACTA2)	2.7	2.5	1	3	8	1.1E−32	20.67	gi|71895043	42.0/30.65
325	Tubulin, beta 2B (TUBB2B)	−3.3	−1.1	1.6	12	63	2.0E−139	106.89	gi|52138699	49.9/56.70
1755	Lamin B2 (LMNB2)	IN	IN	IN	8	24	4.3E−54	45.33	gi|45384202	67.9/40.33
1426	Lamin B2 (LMNB2)	3.1	IN	1.3	7	19	4.7E−60	48.54	gi|45384202	67.9/40.65
Protein translation and elongation										
1763	Eukaryotic translation elongation factor 2 (EEF2)	IN	IN	1.9	9	23	9.9E−81	46.07	gi|45382453	95.4/33.69
612	Eukaryotic translation elongation factor 2 (EEF2)	3.2	1.1	1.5	8	19	4.3E−93	57.94	gi|45382453	95.4/34.01
1782	Acidic ribosomal phosphoprotein (RPLP0)	REP	1	AB	6	31	7.6E−56	39.02	gi|45384494	34.3/36.14
RNA processing										
1626	Heterogeneous nuclear ribonucleoprotein A2/B1 (HNRNPA2B1)	IN	IN	AB	1	4	5.9E−10	7.72	gi|71896753	36.8/23.05
1631	PREDICTED: heterogeneous nuclear ribonucleoprotein A3 (HNRNPA3)	3.6	2.3	−1.8	3	17	1.1E−19	9.52	gi|118093536	39.6/29.05
541	Heterogeneous nuclear ribonucleoprotein H3 (2H9) (HNRNPH3)	−3.7	−1.4	1.3	7	38	8.9E−69	45.22	gi|60302824	36.5/36.50
Ubiquitin–proteasome pathway, antigen processing and presentation and proteolysis										
769	Ubiquitin carboxyl-terminal esterase L3 (UCHL3)	−2.5	−1.5	−1.4	2	14	4.9E−17	14.20	gi|45382251	26.3/28.34
710	Proteasome (prosome, macropain) subunit, beta type, 7 (PSMB7)	REP	−1.3	1.1	2	13	2.1E−15	12.47	gi|45383366	29.9/30.78
1576	PREDICTED: similar to mSUG1 protein (PSMC5)	REP	AB	2.6	2	19	3.3E−24	13.53	gi|118102836	45.6/47.87
1171	Cathepsin D (CathD)	2.8	2	2.5	2	13	1.0E−14	8.96	gi|45384002	43.3/13.30
1747	Cathepsin D (CathD)	2	2.5	1.8	1	7	2.8E−10	6.57	gi|45384002	43.3/28.46
494	Cathepsin D (CathD)	REP	−1.2	−1.9	1	7	1.8E−10	5.32	gi|45384002	43.3/39.21
1569	MHC class II alpha chain (B-LA)	−3.6	1	−1.3	1	14	0.00099	3.33	gi|118099043	28.0/32.14
Signal transduction										
1609	PREDICTED: similar to D4-GDP-dissociation inhibitor (D4-GDI)	5.3	1.6	−1.3	1	4	0.00745	2.26	gi|50728568	23.0/18.40
775	PREDICTED: similar to D4-GDP-dissociation inhibitor (D4-GDI)	−2.7	−2.5	−1.6	5	49	2.3E−77	51.21	gi|50728568	23.0/27.15
1174	Membrane associated guanylate kinase, WW and PDZ domain containing (MAGI3)	6.3	2.7	3.4	1	3	0.00043	2.40	gi|60593020	12.2/13.70
583	Guanine nucleotide binding protein (G protein), beta polypeptide 1 (GNB1)	−2	−1.2	−1.2	1	8	6.3E−21	9.42	gi|61098210	37.3/35.15
Transport										
1125	Transthyretin (TTR)	REP	−1.1	REP	1	11	4.0E−05	2.96	gi|45384444	16.3/15.28
1607	Alpha 2 globin (HBA2)	2.8	1	−1.3	9	85	1.9E−95	76.78	gi|52138645	15.7/27.34
1155	Fatty acid binding protein 4, adipocyte (FABP4)	REP	AB	AB	5	56	4.7E−46	29.37	gi|45383556	14.8/14.55
1143	Fatty acid binding protein 3 (FABP3)	1.2	IN	IN	3	80	4.2E−87	50.64	gi|71894843	14.8/14.80
1605	PREDICTED: similar to voltage-gated sodium channel type II alpha subunit (SCN2A)	IN	AB	AB	1	2	0.00661	3.15	gi|118093616	25.5/32.35
Cell proliferation, differentiation and DNA repair										
598	Proliferating cell nuclear antigen (PCNA)	−1.6	1.4	2.7	6	46	3.1E−45	29.16	gi|45383776	28.9/34.36
1781	Nucleophosmin 1 (NPM1)	3.2	1.1	1.5	1	6	1.1E−14	8.85	gi|45383996	32.6/20.09
1040	Stathmin 1/oncoprotein 18 (STMN1)	REP	1	IN	1	13	1.0E−09	5.36	gi|50053682	17.1/18.67

(continued on next page)

Table 1 (*continued*)

Ref. spot no.	Protein name[a]	Fold change in expression			Number of peptides identified	Protein coverage[b] (%)	Probability	Protein score[c]	Accession no.	Mr. (predicted/ observed) (kDa)
		7 dpi	14 dpi	21 dpi						
Enzymes										
1769	Triosephosphate isomerase 1 (TPI1)	IN	AB	AB	2	13	5.0E−08	5.76	gi|45382061	26.6/27.19
789	Triosephosphate isomerase 1 (TPI1)	−2.3	−1.5	−1.4	3	18	4.5E−25	22.54	gi|45382061	26.6/27.26
1604	PREDICTED: aldolase B, fructose-bisphosphate (ALDOB)	5.2	2.7	2.6	1	2	1.9E−05	4.90	gi|50761947	39.3/38.76
1629	PREDICTED: aldolase B, fructose-bisphosphate (ALDOB)	−5.4	−1.6	1	1	2	0.00261	2.48	gi|50761947	39.3/39.68
791	Glutathione-S-transferase theta 1 (GSTT1)	−1.4	REP	1	1	13	0.00015	2.41	gi|45382479	29.8/27.14
1596	Phosphoglycerate mutase 1 (brain) (PGAM1)	−4.9	1	IN	10	83	4.1E−169	95.00	gi|71895985	28.9/29.17
283	Amylase, alpha 2A; pancreatic (AMY2A)	−3.5	−1.3	−5.7	13	72	3.9E−180	120.50	gi|47825395	57.5/58.61
Protein folding/stress response										
1702	Heat shock cognate 70 (HSC70)	IN	AB	AB	9	31	2.3E−141	87.04	gi|45384370	70.8/66.08
1603	Heat shock protein 70 (HSP70)	IN	AB	REP	2	6	1.5E−27	16.43	gi|55742654	69.7/40.14
1735	Heat shock protein 70 (HSP70)	IN	REP	REP	3	10	6.7E−25	18.12	gi|55742654	69.7/69.27
Antioxidant										
1527	PREDICTED: similar to natural killer cell enhancing factor isoform 4 (NKEF)	6.3	2	1.2	7	49	5.1E−78	60.88	gi|50751518	22.1/24.61
1606	PREDICTED: similar to natural killer cell enhancing factor isoform 4 (NKEF)	IN	IN	IN	6	48	4.6E−113	86.61	gi|50751518	22.1/23.77
Other										
1753	Cadherin 4, type 1, R-cadherin (retinal) (CADH4)	IN	AB	AB	1	5	0.000240	2.68	gi|52138677	100.8/26.5
1427	Serine (or cysteine) proteinase inhibitor, clade B (ovalbumin), member 6 (SERPINB6)	REP	−1.4	−2.7	4	19	5.2E−33	19.89	gi|57530448	42.9/40.60
917	Ferritin, heavy polypeptide 1 (FTH1)	AB	1.2	REP	3	30	3.8E−38	19.77	gi|45384172	21.1/21.64
1612	Myosin regulatory light chain 9 (MYL9)	IN	1.9	1.3	1	7	5.6E−08	5.76	gi|45384118	19.8/21.52
968	Myosin regulatory light chain, isoform L20-B (MYLL20B)	−2.3	1	REP	2	15	2.7E−12	8.38	gi|45384410	19.8/20.42
704	Transglutaminase 4 (prostate) (TGM4)	8	−1.3	−1.1	7	15	3.8E−84	56.85	gi|57530757	78.8/30.85
111	Transglutaminase 4 (prostate) (TGM4)	−2.7	−2.5	−1.6	9	24	8.2E−121	65.80	gi|57530757	78.8/89.70
Hypothetical proteins										
1765	PREDICTED: hypothetical protein (HP1)	IN	AB	AB	2	19	5.0E−17	8.34	gi|50731161	34.5/35.40
585	PREDICTED: hypothetical protein (HP2)	−2.3	1	−1.2	3	15	6.3E−29	19.97	gi|50745642	34.8/34.74
1655	PREDICTED: hypothetical protein (HP3)	REP	REP	REP	1	5	9.7E−05	1.12	gi|50761148	38.4/22.29
347	PREDICTED: hypothetical protein, partial (HP4)	IN	1	1.8	8	16	3.8E−54	44.03	gi|118093732	51.7/55.78
1610	PREDICTED: hypothetical protein (HP5)	2.2	2.8	3.7	1	3	1.2E−07	6.58	gi|118086389	32.8/20.78

IN = induced, detected only in infected group, REP = repressed, detected only in the control group, AB = absent in both groups, dpi = days post-infection.

[a] Protein abbreviations are in parentheses.

[b] Protein coverage = (total amino acids in detected peptides / total amino acids in peptides detectable by mass spectrometer) × 100 (see Materials and methods section for details).

[c] Protein score is the sum of Xcorr values obtained from Bioworks analysis.

200 μg of total proteins. The molecular weights of spots ranged from 8 to 120 kDa. Differences in spot intensity were identified as either qualitative or quantitative changes (Figs. 1 and 2). On average there were over 500 spots on each gel, however only 309, 375 and 341 spots from each group at consecutive sampling points were considered for statistical comparison. Because, according to our selection criteria, only those spots which were present in at least 3 of 4 gels in both infected and control groups at a given sampling point were considered for quantitative comparisons. The highest number of qualitative differences in spots was detected at 7 dpi ($n=26$). This number decreased in the subsequent sampling time point at 14 dpi ($n=19$) and the lowest number was at 21 dpi ($n=7$). Although a similar pattern was seen in the total number of spot differences, the highest number of quantitatively significant differences (false discovery rate or FDR ≤ 0.05 and fold change ≥ 2) in spot expression was detected at 7 dpi ($n=33$), which was followed by 21 dpi ($n=12$) and 14 dpi ($n=2$). Among these spots, there were 16, 1 and 5 spots identified as significantly up-regulated at 7, 14 and 21 dpi, respectively. The rest were significantly down-regulated (Fig. 3). Taken together, 61 protein spots were detected as either quantitatively or qualitatively differentially expressed at least once during different sampling points.

Identification of differentially expressed proteins by mass spectrometry

In order to obtain the identities of the differentially expressed spots, the spots were manually excised from preparative gels prepared by loading 1 mg of total proteins and staining with Coomassie blue. Subsequently, trypsin-digested spots were identified by 1D LC ESI MS/MS. Peptide identities with FDR < 0.01 were considered significant and, in total, the identity of proteins in 61 different spots representing 48 different proteins was determined (Table 1). Moreover, several spots contained peptides generated from multiple proteins. While we have used the protein with the highest relative abundance under corresponding spot number throughout our discussion, the complete list of spots with multiple identities has been provided as supplementary Table 1.

Several proteins were differentially expressed at more than one time point, e.g. cathepsin D (CathD), natural killer cell enhancing

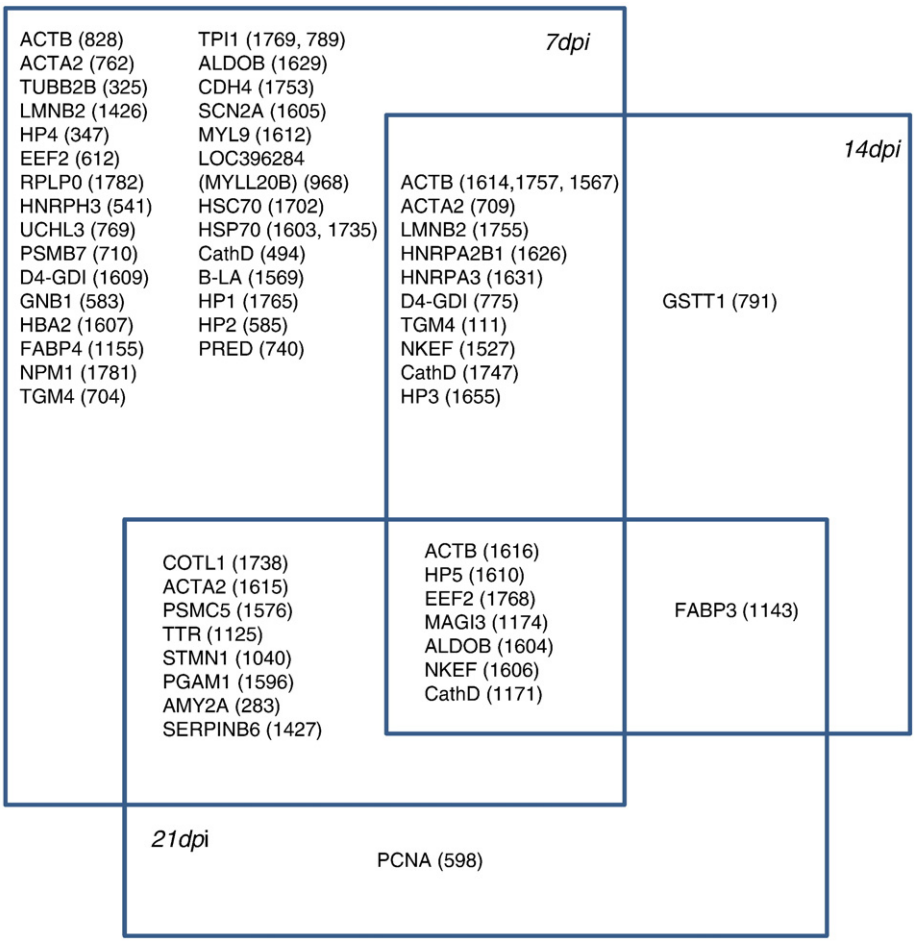

Fig. 4. Venn diagram summarizing the spots that were significantly differentially expressed in the spleen tissues of MDV-infected chickens according to their corresponding time of sampling. These identities include both quantitatively and qualitatively differentially expressed spots. The identities of spots which were commonly expressed were placed in overlapping areas accordingly. Corresponding spot numbers are in parentheses. Refer to Table 1 for the respective protein names.

factor isoform 4 (NKEF), eukaryotic elongation factor 2 (EEF2), aldolase B (ALDOB), membrane associated guanylate kinase (MAGI3), a predicted hypothetical protein (HP5) and beta actin (ACTB) at all three times. In total, 30 proteins were differentially expressed exclusively at 7 dpi. Notably, several proteins involved in antigen presentation pathways, the ubiquitin–proteasome protein degradation system and a number of spots representing several cellular structural proteins were among those that were differentially

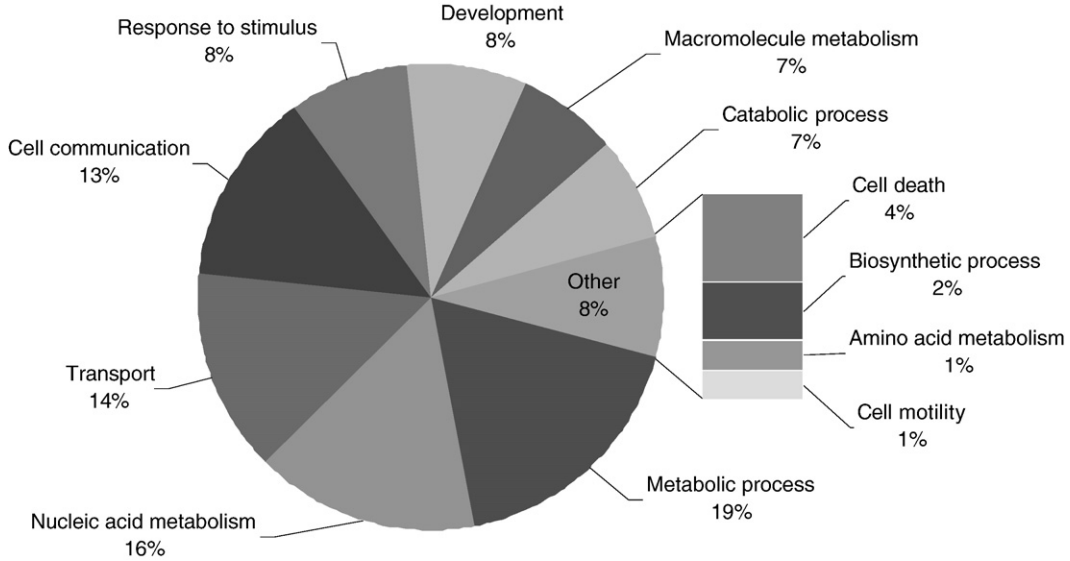

Fig. 5. Gene Ontology analysis of significantly changed proteins according to their biological process. This classification was produced based on the analysis using GOSlimViewer tool at Agbase database (http://www.agbase.msstate.edu/) as described in the Materials and methods section.

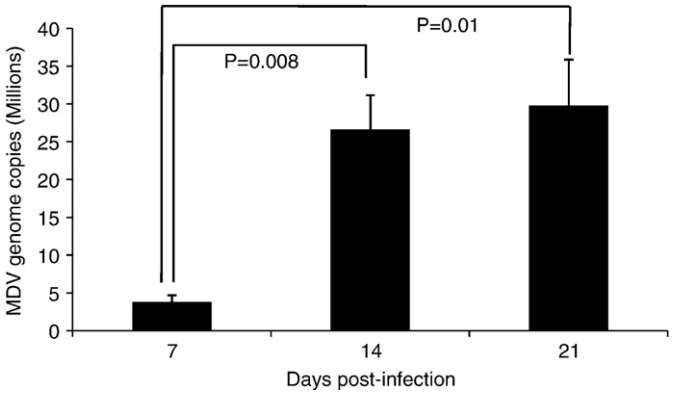

Fig. 6. MDV genome load in infected spleens. Chickens were infected with the RB1B strain of MDV and sampled at 7, 14 and 21 days post-infection. Meq copy numbers in 100 ng of spleen DNA were quantitated using real-time PCR. At least three spleen samples were analyzed in duplicate at each sampling time point. The error bars represent standard error of the mean.

expressed exclusively at 7 dpi. There was only one spot specific to each of 14 and 21 dpi. These spots were identified as glutathione-S-transferase theta 1 (14 dpi) and proliferating cell nuclear antigen (21 dpi). The significant changes detected with the rest of the spots overlapped between each time point in varying numbers.

Interestingly, some of the spots representing a particular protein showed opposite directions of regulation even within the same group. For example, three spots with different molecular weights and p*I* were identified as CathD (Table 1). Of these three spots, two spots with molecular weights of 13.3 and 28.4 kDa were found to be up-regulated in infected birds at more than one time point. The summarized distribution of the identities of spots identified at each time point is presented in Fig. 4.

Gene Ontology annotation

Forty-percent of the identified proteins were associated with the cytoplasm and the plasma membrane (terms GO:0005737 and GO:0005886 respectively). Furthermore, there were 24% nuclear and nuclear envelope proteins (GO:0005634 and GO:0005635), 22% cytoskeleton-associated proteins (GO:0005856) and 5% extracellular proteins (GO:0005576). Nine-percent of proteins did not have any GO annotation with respect to their cellular compartment, hence, were categorized very broadly as being associated as a "cellular component" (GO:0005575). For biological processes, the highest associations (18%) were with metabolic processes (GO:0008152). Another 16% associations were with nucleic acid metabolism (GO:0006139), while 14% and 13% were associations with transport (GO:0006810) and cell communication (GO:0007154), respectively. Among the remaining associations, 4% were associated with cell death (GO:0008219) (Fig. 5).

Determination of MDV genome load in infected spleens

Virus genome copy numbers in infected spleens were determined using quantitative real-time PCR (qPCR). Using conventional PCR screening, MDV-Meq gene could be amplified from DNA of all infected spleens but not from any of the uninfected controls (data not shown). Results of the subsequent qPCR analysis of infected samples are presented in Fig. 6. The average MDV-Meq copy numbers were $3.82\times10^6\pm1.48\times10^6$ ($n=3$), $2.66\times10^7\pm7.78\times10^6$ ($n=3$) and $2.98\times10^7\pm1.22\times10^7$($n=4$) per 100 ng of spleen DNA at 7, 14 and 21 dpi, respectively (Fig. 6). There was a statistically significant difference between genome copy numbers at 7 dpi compared to other time points.

Discussion

In the present study, we have profiled the global protein expression changes in the chicken spleen in response to MDV infection at various time points representing the different phases of MDV life cycle. Furthermore, we have determined the identity of the spots that were differentially expressed between infected and uninfected birds using mass spectrometry.

Among the 48 proteins that were differentially expressed, there was considerable number of proteins that had multiple spots in 2D gels. In addition, there was some degree of disagreement between the expected and experimental molecular weights in case of some of the proteins. This could be due to several reasons. First, some proteins exist as different isoforms (therefore different p*I*) as well as different intermediate stages between translation and functionally mature form (i.e. pre-pro- and pro-forms of protein). This could change the molecular weight and/or the isoelectric point (for example, please see the discussion regarding different spots of CathD below). Another reason is possible protein degradation between sample collection and processing. Interestingly, no protein with multiple matches showed any specific migration pattern in our 2D gels (such as trains of spots). While current data are not enough to determine the exact reason for such discrepancies, it should be noted that several previous studies using 2D gels have also reported the presence of similar patterns of proteins with multiple spots (Dupont et al., 2008; Liu et al., 2008; Saldanha et al., 2008; Zheng et al., 2008).

Analysis of viral load in spleen tissue revealed a significant increase over time. Although viral genome load may not be a direct indicator for the degree of infection, there is a correlation between MDV genome load and the number of infected cells (Bumstead et al., 1997) as well as with subsequent MD incidence (Islam et al., 2006) or protection conferred by vaccines against MD (Abdul-Careem et al., 2007). Based on our previous observations, virus genome load of around 1×10^5 copies/100 ng of spleen DNA is correlated with development of tumors in infected birds (Abdul-Careem et al., 2007). Therefore, it is conceivable that the virus copy numbers observed in the present study would be an indicative of a high level of infection.

The proteins identified in the present study are involved in a variety of cellular processes, notably the antigen processing and presentation, ubiquitin–proteasome protein degradation, formation of the cytoskeleton, cellular metabolism, signal transduction and regulation of translation (Table 1). The significance of these processes in chicken-MDV interaction is discussed below. Although this was not determined in the present study, temporal changes in the cellular composition of the spleen may have, at least in part, influenced the whole spleen organ proteome. However, the advantage of our method is that the proteins that are differentially expressed could be used to point to cell subsets and/or mechanisms that have a potential involvement in MDV–host interactions and could be targeted for future studies.

Effects of MDV infection on the ubiquitin–proteasome pathway and MHC antigen presentation

Among the differentially expressed spots, several proteins were identified that are either directly or indirectly involved in the ubiquitin–proteasome (UPP) and antigen presentation pathways (Table 1). In our study, we identified three differentially regulated proteins, namely ubiquitin C-terminal hydrolase L3 (UCHL3), proteasome (prosome, macropain) subunit beta type 7 (PSMB7) and predicted protein similar to mouse proteasome 26S subunit ATPase 5 (PSMC5) (also known as mSUG1), which are involved in UPP (Table 1). Among them, chicken UCHL3 (alias UCH-6) has 86% amino acid similarity with its human counterpart (Baek et al., 1999), which is a deubiquitinating enzyme (DUB) that functions as a negative regulator of ubiquitination of proteins as well as facilitates recycling of

ubiquitin. Increasing evidence suggests that DUBs are important regulators of many cellular processes such as endocytosis, apoptosis and various signalling pathways (Wing, 2003). Several virus-encoded proteins such as Epstein–Barr virus (EBV)-encoded Epstein–Barr nuclear antigen 1 and herpes simplex virus (HSV-1) regulatory protein ICP0 have been shown to interact with DUBs for viral survival in infected cells (reviewed in Lindner, 2007). Although there is a high amino acid identity between human UCH-L3 and chicken UCH-6, they differ with respect to their substrate specificity and tissue distribution (Baek et al., 1999). Therefore, the chicken ortholog of UCH-L3 may not have a similar role in viral infections. More functional studies are needed to understand the significance of the down-regulation of UCHL3 in MDV infection.

Down-regulation of PSMB7 at 7 dpi probably indicates the modification of proteasome into immunoproteasome under the influence of interferon (IFN)-γ to enhance the generation of peptides for binding to major histocompatibility complex (MHC) class I molecules. In this process, three constitutive beta subunits of the 20S proteasome, namely delta, X and Z (PSMB7), are replaced by IFN-γ inducible low molecular mass peptide (LMP)-7, LMP-2 and multi-catalytic endopeptidase complex-like (MECL) catalytic subunits, respectively (Griffin et al., 1998). Although we could not detect up-regulation of IFN-γ inducible subunits, given the reciprocal regulation between constitutive and IFN-γ inducible subunits (Hisamatsu et al., 1996), down-regulation of PSMB7 may indicate the effect of induced IFN-γ. In line with that, MDV is known to induce IFN-γ in chickens as early as 3 dpi and remains up-regulated until at least 15 dpi (Xing and Schat, 2000). Moreover, although MDV is capable of down-regulating MHC-I expression *in vitro*, elevated IFN-γ has been shown to reverse the effect of MDV on MHC-I (Levy et al., 2003). Our present observations do not provide evidence for differential regulation of MHC-I expression. However, given the possible enhancement of immunoproteasome activity, it is conceivable that there is an enhanced MHC-I-mediated antigen presentation.

The 19S proteasome subunit SUG1 up-regulates MHC-II expression by interaction with class II transactivator (CIITA) gene and MHC-II proximal promoter in human. MHC-II expression is reduced in the absence of the expression of SUG1 (Bhat et al., 2008). In agreement with this, the observed absence of predicted protein, mSUG1 in infected birds is associated with a significant decrease in the expression of the MHC class II alpha chain (B-LA) in infected spleens at 7 dpi. Reduction of the MHC-II expression is known to be a predominant way of evading the host immune response by a number of viruses including herpesviruses (Hegde et al., 2003). In agreement with our present observation of down-regulation of MHC-II expression, previous work from our laboratory showed that MDV infection causes significant down-regulation of invariant (Ii) chain gene expression in the chicken spleen tissue (Sarson et al., 2006). In contrast to this observation, Niikura et al. (2007) have shown an up-regulation of MHC-II in bursa cells of chickens infected with Md11, another very virulent strain of MDV. However, in contrast to our present infection model which used outbred SPF chickens, they have used chickens from a cross between two inbred lines, $15I_5$ and 7_1, both of which are susceptible to MD (Bacon et al., 2000). Therefore, it is possible that the difference in genetic background of infected birds may have, at least in part, contributed to these contradicting observations.

Taken together, our observations suggest that there is enhanced antigen processing, presumably mediated by elevated IFN-γ for MHC class I pathway, while there is a down-regulation of MHC class II-mediated antigen presentation at least in our experimental model at early stages of the disease.

Alterations in the proteins associated with the cytoskeleton network

In the current study, altered spot profiles were observed for a number of cytoskeleton-associated proteins representing all three main categories of cytoskeleton proteins, namely microfilaments, intermediate filaments and microtubules. Among the microfilament proteins, all detected actin spots, except for alpha-2 actin (ACTA2) and a predicted protein similar to coactosin-like 1 (COTL1) at 21 dpi, were either newly induced or significantly up-regulated across the experimental period. Intermediate filament, lamin B2 (LMNB2) spots also were either up-regulated or newly induced in infected birds at all times. However, microtubule protein, tubulin β 2B (TUBB2B) was significantly down-regulated in infected birds at 7 dpi (Table 1).

Changes in cytoskeleton proteins have been previously described in several other viral infections, such as IBDV (Zheng et al., 2008), severe acute respiratory syndrome (SARS)-associated coronavirus (Jiang et al., 2005) and human papillomavirus type 8 (Akgül et al., 2009). Herpesviruses are known to interact with the actin filament system and its regulatory protein, Rho GTPase, at various stages of infection (Favoreel et al., 2007). In addition to actins, here we have identified a Rho GTPase regulatory protein, D4-GDI, as a protein that was differentially expressed in spleen of infected chickens (discussed in detail elsewhere in the Discussion). This may indicate a putative role of the same system in the context of MDV infection. Schumacher et al. (2005) showed that MDV-encoded US3 ortholog protein causes depolymerization of the actin stress fibers. However, its role in MDV replication and/or spreading is still unclear. Stathmin 1 (STMN1), which also plays a role in the regulation of the microtubule system, has been shown to be up-regulated in EBV-infected B lymphocytes in human as early as 7 dpi (Baik et al., 2007). In the present study, we could not detect changes in STMN1 in spleen at 7 dpi. However, the expression of this protein was induced by 21 dpi. As a possible result of regulation by STMN1, TUBB2B, which is a component of the microtubule filament system, also showed a similar pattern of expression in MDV-infected spleen tissues. However, if that change has any direct relationship with the STMN1 is not known. Apart from its interaction with the microtubule system, STMN1 has been shown to interact with heat shock protein 70 (HSP70) proteins, particularly with heat shock cognate 70 (HSC70) (Manceau et al., 1999). In line with that, we have also identified significant changes in the expression of HSP70 proteins, including HSC70.

Another cellular structural protein, LMNB2, which is associated with the nuclear membrane, was up-regulated in infected birds throughout the experimental period as a probable result of the egress process of virus nucleocapsids from the infected nuclei. The nucleocapsids of herpesviruses acquire a temporary envelope from the inner nuclear membrane before egress by budding off from the infected cell nuclei (Granzow et al., 2001). In line with that, Camozzi et al. (2008) have reported various biochemical and structural modulations, including mislocalization of lamin proteins in the nuclear envelope of cells infected with human cytomegalovirus. Although Camozzi et al. (2008) did not observe any quantitative changes in the expression of lamin proteins, qualitative changes in the expression of the same protein have been described in infections with several other viruses such as IBDV (Zheng et al., 2008), enterovirus 71 (Leong and Chow, 2006) and SARS-associated coronavirus (Jiang et al., 2005). Similar to the other members of the family, MDV particles egress from the nucleus of infected cells through budding (Baigent and Davison, 2004). Therefore, it is conceivable that the up-regulation of LMNB2 protein observed in the present experiment is, at least partly, the result of such interaction.

Mixed cell populations undergoing activation/proliferation as well as apoptosis

Proliferating cell nuclear antigen (PCNA), which is one of the critical proteins in cell survival, was significantly up-regulated in infected spleens at 21 dpi. PCNA is an essential component in DNA synthesis process in the cell. Therefore, it is likely that induction of PCNA represents highly replicating cell populations in the spleen at

21 dpi. While it is possible that elevated PCNA expression represents a transformed cell population, possible interactions between PCNA and viral proteins might be also occurring. For example, HSV-1 encoded protein, ICP34.5, interacts with PCNA of infected cells, presumably preventing virus-induced translational arrest (Brown et al., 1997; Harland et al., 2003). The possibility of a yet unidentified MDV protein interacting with PCNA remains to be investigated.

ICP34.5 has also been shown to interact with phosphatase 1, preventing the inactivation of eukaryotic elongation factors (EEF), a group of proteins which play an important role in protein biosynthesis, hence being important in various cell processes including proliferation (Thompson and Sarnow, 2000). EEF2 was among the proteins that were up-regulated at both 7 and 14 dpi. Increased levels of EEF2 have been shown in response to human immunodeficiency virus (HIV) protein, Vpr, and have been shown to have the potential of preventing Vpr-mediated apoptosis in CD4+ T cells (Zelivianski et al., 2006). D4-GDP-dissociation inhibitor (D4-GDI) (also known as Ly-GDI) was differentially regulated in infected birds compared to uninfected controls. As mentioned above, Ly-GDI represents a group of proteins i.e. GDI, which are involved in the regulation of another group of proteins, Rho family GTPases. Apart from its involvement in the organization of the cytoskeleton, Rho-GTPases are also involved in cell signalling and proliferation. GDIs are involved in the regulation of shifting of Rho GTPase between the active GTP-bound form and the inactive GDP-bound form. Our present observations showed a more than 5-fold increase of an 18.4 kDa D4-GDI spot while there was a significant decrease of the presumably intact protein of 27 kDa. While activation as well as apoptosis of different types of cells in response to viral infections has been well documented, our present observations may highlight some of the molecules involved in these processes in the context of MDV infection.

Cathepsin D (CathD), a lysosomal aspartic proteinase, was among the proteins that were differentially expressed in infected spleens at all three time points. There were two spots with molecular weight of approximately 13 and 28 kDa which were up-regulated, while another one (39.2 kDa) was down-regulated. CathD is synthesized as a single chain pre-pro-enzyme and after being cleaved into several successive intermediates, it forms the mature 34 + 14 kDa form consisting of a heavy and a light chain in the lysosome (Laurent-Matha et al., 2006). Therefore, processing of the 39.2 kDa intermediate into the mature enzyme appears to be induced by MDV infection. CathD has been shown to be an important mediator of apoptosis induced through the lysosomal pathway (Guicciardi et al., 2004). While CathD appears to be involved in the intrinsic pathway of the induction of apoptosis in activated T lymphocytes in human (Bidere et al., 2003), it may also play a significant role in the resolution of inflammation by inducing apoptosis in neutrophils (Conus et al., 2008). Apart from its role in the induction of apoptosis, increasing evidence suggests that CathD plays a significant role in cancer progression and metastasis. In the context of MD, several studies have shown the occurrence of cell death in MDV-infected organs such as the bursa of Fabricius (St Hill and Sharma, 1999), thymus (Morimura et al., 1996) and in peripheral blood mononuclear cells (Morimura et al., 1995). While it is conceivable that up-regulated CathD may play a role in apoptosis during the early stages of MD, it may also have a role in T cell transformation in the later stages of the disease; however, this needs to be further studied.

Transglutaminase 4 (TGM4) is among the proteins with the highest fold increase in spleens of infected chickens. Generally, transglutaminases are involved in post-translational modification of proteins (Beninati and Piacentini, 2004). TGM4 is highly expressed in the prostate gland of humans but little information is available about the function of this protein in chickens. TGM2, which is a ubiquitously expressed protein in human (also known as tissue TGM, tTGM), has been shown to play a significant role in stress response (Ientile et al., 2007) notably in apoptotic cell death. While TGM2 is up-regulated in apoptotic cells, it acts as a molecular glue and appears to stabilize the dying cells to prevent release of intracellular molecules prior to clearance by phagocytosis (Fesus and Szondy, 2005) thereby preventing adverse effects, such as excessive inflammatory reactions. Assuming chicken TGM4 has a similar role as that of human TGM2, above observations may explain the putative role of the former in the context of host–MDV interactions in the spleen to prevent collateral damage to the neighbouring cells.

Enhancement of cellular metabolic process

According to GO classification based on the biological process, the highest association of identified proteins in the current study was with metabolic processes (19%) (Fig. 5). Notably, several metabolic enzymes associated with glycolysis have been found differentially regulated. Among them, a 38.76 kDa spot representing aldolase B fructose-bisphosphate (ALDOB) was constantly up-regulated in infected spleens at all time points. Interestingly, another spot with similar identity and molecular weight but slightly different p*I* was significantly down-regulated only at 7 dpi. While different p*I*s for the same protein is possible with structural changes such as phosphorylation, functional relevance in this context needs to be elucidated. Another two newly induced glycolytic enzymes, each at 7 and 21 dpi, were identified as triosephosphate isomerase 1 (TPI1) and phosphoglycerate mutase 1 (PGAM1), respectively. Viruses utilize host cell metabolic process for their replication process. In agreement with the present observations, significantly elevated levels of several serum enzymes, including aldolase B, in response to MDV infection *in vivo* has been previously described (Ivanov et al., 1974). Further, MDV-encoded protein pp38 has been shown to up-regulate cellular metabolic activities *in vitro* as determined by the enhanced activity of mitochondrial dehydrogenases (Li et al., 2006). Similarly, human cytomegalovirus infection in fibroblasts has also shown overall up-regulation of a number of glycolytic enzymes (Munger et al., 2006).

In conclusion, findings of the present study highlight some of the mechanisms involved in the host response in the spleen to MDV infection during various time points representing different stages of MDV pathogenesis. Although the functions of the proteins, which were identified here, were not studied, it is likely that all or some of them are involved in host–virus interactions. One of the limitations of the tools used in this study is the inefficiency of detecting low abundance proteins or those with low molecular weights, such as cytokines and chemokines. Therefore, a more comprehensive study is needed to elaborate on our present observations and to further explore other proteins that may play a role in pathogenesis of the virus as well as host responses to this virus.

Materials and methods

Experimental animals

All the chickens used in this experiment were one-day old specific pathogen free (SPF) chickens obtained from the Animal Disease Research Institute, Canadian Food Inspection Agency (Ottawa, Ontario, Canada). Birds were kept in an isolation facility at the Ontario Veterinary College throughout this experiment.

Infection virus strain

Chickens were infected with the RB1B strain of very virulent Marek's disease virus (passage 9) (Schat et al., 1982) which was obtained from Dr. K.A. Schat (Cornell University, NY, USA).

Experimental design

Twenty-four, one-day old chicks were randomly divided into two groups and were housed in the isolation facility. One group of birds

($n=12$) was given 750 plaque-forming units (PFU) of the RB1B strain of very virulent MDV intraperitoneally on day 5 of age. The rest ($n=12$) were kept as uninfected controls. Infected and uninfected control birds were kept in separate units with similar environmental conditions. On 7, 14 and 21 dpi, representing different stages of MDV pathogenesis, four chickens that were randomly selected from each group were euthanized using CO_2 inhalation. At necropsy, a portion of spleen was collected from each bird and was snap-frozen in liquid nitrogen. Subsequently, frozen tissues were kept at −80 °C until further processing. Another portion was preserved in RNAlater (Qiagen Inc., Missisauga, ON, Canada). Animal experiments were conducted in accordance with the guidelines provided by the Canadian Council on Animal Care. All experiments complied with institutional animal care guidelines and were approved by University of Guelph Animal Care Committee (protocol number 06R015).

Sample preparation for proteomic analysis

Each frozen spleen tissue was briefly homogenized in a lysis buffer (pH 8.5) containing 30 mM Tris–Cl, 2 M thiourea, 7 M urea and 4% (W/V) CHAPS. The volume of lysis buffer used for each tissue sample was equal to 15 times of tissue mass. Samples were further solubilized by sonication for 5 min on ice and insoluble tissue debris was removed by centrifugation under 18,000 ×*g* at 4 °C. Subsequently, supernatant was collected separately from each sample and protein concentrations were determined using the Bio-Rad Protein Assay as prescribed by the manufacturer.

Two-dimensional polyacrylamide gel electrophoresis (2D-PAGE)

The spleen protein sample from each chicken was analyzed separately. There were a total of 24 chickens in two groups (infected and uninfected) i.e. 24 protein samples for analysis by 2D-PAGE. Each analytical 2D-PAGE gel was prepared with 200 μg of proteins mixed with rehydration buffer (8 M urea, 2% CHAPS, 90 mM DTT, 5 μl/ml appropriate IPG buffer, 12 μl/ml Destreak reagent (GE Healthcare) and 0.005% bromophenol blue) to a total volume of 250 μl. The first dimension separation was performed in 13 cm, pH 3–10 non-linear Immobiline DryStrips (GE Healthcare) using Ettan IPGphor isoelectric focusing unit (GE Healthcare). After rehydration at 30 V for 12 h, isoelectric focusing was performed at 500 V for 1 h, 1000 V for 1 h and 8000 V until a total of 57,000 volt hours was reached. Each focused strip was incubated at room temperature, initially in 10 ml of equilibration buffer (50 mM Tris–Cl (pH8.8), 6 M urea, 30% (v/v) glycerol, 2% (w/v) SDS and 0.005% bromophenol blue) containing 1% (w/v) DTT for 15 min and subsequently in a similar volume of equilibration buffer containing 2.5% (w/v) iodoacetamide for a similar time. For the second dimension separation, each IPG strip was placed on a 12.5% SDS-polyacrylamide gel and four such gels were simultaneously run each time subjecting them to 25 mA/gel of current at 25 °C in a Ruby apparatus until the bromophenol blue dye front reach the opposite edge of the gel. Each gel was subsequently fixed for 1 h in a solution containing 10% (v/v) methanol and 7% (v/v) acetic acid, stained with SYPRO Ruby stain (Bio-Rad) overnight and destained in the fixing solution for 2 h. Gel images were digitized using Typhoon 9400 variable mode imager (GE Healthcare) at 532 nm using a 610 nm filter. Preparative gels were prepared in a similar manner, using 1 mg of protein from each sample and stained them with Coomassie brilliant blue instead of SYPRO Ruby.

Quantification and comparison of protein expression

Digitized gel images were used to estimate the expression of different proteins in each analytical gel using 2004 version of Phoretix 2D software (Nonlinear Dynamics). The pixel volume of each detected spot was referred to as the spot volume and was used in the subsequent comparisons. Background correction for pixel volumes of each spot was done using the mode of non-spot and normalized spot volumes were calculated as a fraction against the total volume of spots in each gel. The spots which were not present in the expected position or showed decreased intensity were considered "down-regulated", while the spots that appeared in only one group or showed enhanced intensity were considered "up-regulated". Although this is an indicator of protein abundance, the possibility of post-translation modifications, hence changes in location of spots on the 2D-PAGE gels, could not be ruled out in our study.

Statistical analysis

There were eight 2D-PAGE gels per time point: 4 derived from infected spleens and 4 from those of uninfected birds. Only the spots that were present in all gels and those that were absent from a maximum of one analytical gel per group at a given time point were considered for the statistical comparison. Statistical analysis was done using SAS (version 9.1). Normalized volumes of each corresponding spot from each group at similar time point were compared with Student *t*-test. The resulting *P* values were used to calculate the FDR. Spots that were having both $P \leq 0.01$ and fold difference >2 in mean normalized volumes were considered as significantly differentially expressed. FDR for any selected spot was less than 5%.

Protein identification

The spots that showed a significant difference, and those expressed only in a particular group at a given sampling point, were selected for identification by 1D LC ESI MS/MS using a LCQ Deca XP Plus mass spectrometer coupled with two Thermo Surveyor MS Pump quaternary gradient pumps at the Life Science and Biotechnology Institute, Mississippi State University as described below.

Each selected spot was excised manually from Coomassie brilliant blue stained preparative gels and "in-gel" digested exactly as previously described (Shevchenko et al., 1996). Proteins were reduced with 5 mM DTT at 65 °C for 5 min and alkylated with 10 mM iodoacetamide at 30 °C for 30 min. Trypsin digestion was done using molecular biology grade porcine trypsin (2 μg; 37 °C; 16 h; 50:1 ratio of protein:trypsin; Promega Corporation, Madison, WI). Liquid chromatography was done with a reverse phase (C18) LC column coupled directly in line with the mass spectrometer. Peptides were loaded into a liquid chromatography gradient ion exchange system containing a Thermo Separations P4000 quaternary gradient pump (ThermoElectron Corporation; San Jose, CA) coupled with a 0.18 × 100 mm BioBasic C18 reverse phase liquid chromatography column of a Proteome X workstation (ThermoElectron). The reverse phase gradient used 0.1% formic acid in acetonitrile and increased the acetonitrile concentration in a linear gradient from 5% to 30% in 15 min and then 30% to 65% in 5 min followed by 95% for 5 min and 5% for 10 min. The mass spectrometer was configured to optimize the duty cycle length with the quality of data acquired by alternating between a single full MS scan followed by three tandem MS scans on the three most intense precursor masses (as determined by Xcalibur software in real time) from the full scan. The collision energy was normalized to 35%. Dynamic mass exclusion windows were set at 2 min and all of the spectra were measured with an overall mass/charge (m/z) ratio range of 300–1700. Identification of all spots was done as a single run in a randomized order. To prevent "carry-over" after the peptides generated from each spot were analyzed, and before those from the next spot were analyzed, the LC column was washed with 95% ACN, a negative control sample was run to confirm no carry-over and the LC column was washed again.

Resulting mass spectra were analyzed using Bioworks 3.2 (ThermoElectron) using a non-redundant proteome database

containing protein from both chicken and MDV-RB1B (build 3.2) downloaded from the NCBI. We used the Bioworks reverse database function to create the decoy database from this proteome database. The probability of the tandem mass spectrometry match occurred by chance was calculated using; (A) the decoy database searching exactly as described by Elias and Gygi (2007) and (B) the orthogonal P(pep) function in Bioworks 3.2 (which calculates probability based on a theoretical *y* and *b* ion spectrum calculated based on theoretical amino acid dissociation). These two probabilities were the used to calculate the FDR as described by Benjamini and Hochberg (1995) and only peptides with FDR<0.01 were considered as a significant and retained for protein identification. The probability of protein identity was then calculated from the peptide probabilities exactly as described (MacCoss et al., 2002; Nesvizhskii et al., 2003). To calculate the percent protein coverage by identified peptides, the protein sequence was digested *in silico* using "*peptidecutter*" (http://us.expasy.org/tools/peptidecutter/ (Gasteiger et al., 2005)) and the total number of amino acids in peptides between 6 and 30 amino acids (the size range of 99% of the peptides detected by the mass spectrometer) was used as the denominator; the peptides identified were used as the nominator. For spots with multiple protein identities, the protein with the highest peptide coverage and highest protein score (i.e. ΣXcorr; a surrogate for the amount of precursor ion) (Nanduri et al., 2005) was considered as the dominant protein and the most likely protein to contribute to the differential expression in the gel. Subsequently, their biological relevance was discussed.

Gene Ontology (GO) analysis

Spot identities were submitted to *GORetriever* (http://www.agbase.msstate.edu/) to obtain the GO annotations. If no annotation was returned, *GOanna* was used to retrieve GO annotations assigned depending on the sequence similarities. The resulting annotations were summarized based on the GOA and whole proteome GOSlim set using *GOSlimViewer* (McCarthy et al., 2006).

Determination of MDV genome load in infected spleen tissues

DNA extraction, conventional PCR confirmation of the presence of MDV-Meq gene and subsequent determination of the absolute MDV genome copy number from infected spleen samples were essentially performed as previously described (Abdul-Careem et al., 2006). Quantitative real-time PCR reactions to determine viral genome load in samples were performed in duplicate.

Acknowledgments

This research was funded by the Natural Sciences and Engineering Research Council of Canada and United States Department of Agriculture NRI 2004-35204-14829. Niroshan Thanthrige-Don is a recipient of a Commonwealth Graduate Scholarship granted by Foreign Affairs and International Trade Canada.

References

Abdul-Careem, M.F., Hunter, B.D., Nagy, E., Read, L.R., Sanei, B., Spencer, J.L., et al., 2006. Development of a real-time PCR assay using SYBR green chemistry for monitoring Marek's disease virus genome load in feather tips. J. Virol. Methods 133, 34–40.

Abdul-Careem, M.F., Hunter, B.D., Parvizi, P., Haghighi, H.R., Thanthrige-Don, N., Sharif, S., 2007. Cytokine gene expression patterns associated with immunization against Marek's disease in chickens. Vaccine 25, 424–432.

Akgül, B., Zigrino, P., Frith, D., Hanrahan, S., Storey, A., 2009. Proteomic analysis reveals the actin cytoskeleton as cellular target for the human papillomavirus type 8. Virology 386, 1–5.

Baaten, B.J.G., Butter, C., Davison, T.F., 2004. Study of host–pathogen interactions to identify sustainable vaccine strategies to Marek's disease. Vet. Immunol. Immunopathol. 100, 165–177.

Bacon, L.D., Hunt, H.D., Cheng, H.H., 2000. A review of the development of chicken lines to resolve genes determining resistance to diseases. Poult. Sci. 79, 1082–1093.

Baek, S.H., Yoo, Y.J., Tanaka, K., Chung, C.H., 1999. Molecular cloning of chick UCH-6 which shares high similarity with human UCH-L3: its unusual substrate specificity and tissue distribution. Biochem. Biophys. Res. Commun. 264, 235–240.

Baigent, S.J., Davison, F., 2004. Marek's disease: an evolving problem. In: Davison, F., Nair, V. (Eds.), Marek's Disease Virus. InBiology and life cycle. Elsevier Academic Press, USA, pp. 62–77.

Baik, S.Y., Yun, H.S., Lee, H.J., Lee, M.H., Jung, S.E., Kim, J.W., et al., 2007. Identification of stathmin 1 expression induced by Epstein–Barr virus in human B lymphocytes. Cell Prolif. 40, 268–281.

Beninati, S., Piacentini, M., 2004. The transglutaminase family: an overview: minireview article. Amino Acids 26, 367–372.

Benjamini, Y., Hochberg, Y., 1995. Controlling the false discovery rate — a practical and powerful approach to multiple testing. J R Stat. Soc. series B Stat. Methodol. 57, 289–300.

Bhat, K.P., Turner, J.D., Myers, S.E., Cape, A.D., Ting, J.P.Y., Greer, S.F., 2008. The 19S proteasorne ATPase Sug1 plays a critical role in regulating MHC class II transcription. Mol. Immunol. 45, 2214–2224.

Bidere, N., Lorenzo, H.K., Carmona, S., Laforge, M., Harper, F., Dumont, C., et al., 2003. Cathepsin D triggers bax activation, resulting in selective apoptosis-inducing factor (AIF) relocation in T lymphocytes entering the early commitment phase to apoptosis. J. Biol. Chem. 278, 31401–31411.

Brown, S.M., MacLean, A.R., McKie, E.A., Harland, J., 1997. The herpes simplex virus virulence factor ICP34.5 and the cellular protein MyD116 complex with proliferating cell nuclear antigen through the 63-amino-acid domain conserved in ICP34.5, MyD116, and GADD34. J. Virol. 71, 9442–9449.

Bumstead, N., Sillibourne, J., Rennie, M., Ross, N., Davison, F., 1997. Quantification of Marek's disease virus in chicken lymphocytes using the polymerase chain reaction with fluorescence detection. J.Virol.Methods 65, 75–81.

Burgess, S.C., 2004. Proteomics in the chicken: tools for understanding immune responses to avian diseases. Poult. Sci. 83, 552–573.

Buza, J.J., Burgess, S.C., 2007. Modeling the proteome of a Marek's disease transformed cell line: a natural animal model for CD30 overexpressing lymphomas. Proteomics 7, 1316–1326.

Buza, J.J., Burgess, S.C., 2008. Different signaling pathways expressed by chicken naive $CD4^+$ T cells, $CD4^+$ lymphocytes activated with staphylococcal enterotoxin B, and those malignantly transformed by Marek's disease virus. J. Proteome Res. 7, 2380–2387.

Camozzi, D., Pignatelli, S., Valvo, C., Lattanzi, G., Capanni, C., Monte, P.D., et al., 2008. Remodelling of the nuclear lamina during human cytomegalovirus infection: role of the viral proteins pUL50 and pUL53. J. Gen. Virol. 89, 731–740.

Conus, S., Perozzo, R., Reinheckel, T., Peters, C., Scapozza, L., Yousefi, S., et al., 2008. Caspase-8 is activated by cathepsin D initiating neutrophil apoptosis during the resolution of inflammation. J. Exp. Med. 205, 685–698.

Dupont, A., Chwastyniak, M., Beseme, O., Guihot, A.L., Drobecq, H., Amouyel, P., et al., 2008. Application of saturation dye 2D-DIGE proteomics to characterize proteins modulated by oxidized low density lipoprotein treatment of human macrophages. J. Proteome Res. 7, 3572–3582.

Elias, J.E., Gygi, S.P., 2007. Target-decoy search strategy for increased confidence in large-scale protein identifications by mass spectrometry. Nat. Methods 4, 207–214.

Favoreel, H.W., Enquist, L.W., Feierbach, B., 2007. Actin and rho GTPases in herpesvirus biology. Trends Microbiol. 15, 426–433.

Fesus, L., Szondy, Z., 2005. Transglutaminase 2 in the balance of cell death and survival. FEBS Lett. 579, 3297–3302.

Gasteiger, E., Hoogland, C., Gattiker, A., Duvaud, S., Wilkins, M.R., Appel, R.D., et al., 2005. The proteomics protocols handbook. In: Walker, J.M. (Ed.), Protein Identification and Analysis Tools on the ExPASy Server. InHumana Press, pp. 571–607.

Granzow, H., Klupp, B.G., Fuchs, W., Veits, J., Osterrieder, N., Mettenleiter, T.C., 2001. Egress of alphaherpesviruses: comparative ultrastructural study. J. Virol. 75, 3675–3684.

Griffin, T.A., Nandi, D., Cruz, M., Fehling, H.J., Kaer, L.V., Monaco, J.J., et al., 1998. Immunoproteasome assembly: cooperative incorporation of interferon gamma (IFN-gamma)-inducible subunits. J. Exp. Med. 187, 97–104.

Guicciardi, M.E., Leist, M., Gores, G.J., 2004. Lysosomes in cell death. Oncogene 23, 2881–2890.

Gygi, S.P., Rochon, Y., Franza, B.R., Aebersold, R., 1999. Correlation between protein and mRNA abundance in yeast. Mol. Cell. Biol. 19, 1720–1730.

Harland, J., Dunn, P., Cameron, E., Conner, J., Brown, S.M., 2003. The herpes simplex virus (HSV) protein ICP34.5 is a virion component that forms a DNA-binding complex with proliferating cell nuclear antigen and HSV replication proteins. J. Neurovirol. 9, 477–488.

Hegde, N.R., Chevalier, M.S., Johnson, D.C., 2003. Viral inhibition of MHC class II antigen presentation. Trends Immunol. 24, 278–285.

Hisamatsu, H., Shimbara, N., Saito, Y., Kristensen, P., Hendil, K.B., Fujiwara, T., et al., 1996. Newly identified pair of proteasomal subunits regulated reciprocally by interferon gamma. J. Exp. Med. 183, 1807–1816.

Ientile, R., Caccamo, D., Griffin, M., 2007. Tissue transglutaminase and the stress response. Amino Acids 33, 385–394.

Islam, A.F.M.F., Walkden-Brown, S.W., Islam, A., Underwood, G.J., Groves, P.J., 2006. Relationship between Marek's disease virus load in peripheral blood lymphocytes at various stages of infection and clinical Marek's disease in broiler chickens. Avian Pathol. 35, 42–48.

Ivanov, V., Bozukova, T., Nikolova, M., 1974. Changes in the activity of several serum enzymes in chicks with Marek's disease. Vet. Med. Nauki 11, 18–24.

Jiang, X.S., Tang, L.Y., Dai, J., Zhou, H., Li, S.J., Xia, Q.C., et al., 2005. Quantitative analysis of severe acute respiratory syndrome (SARS)-associated coronavirus-infected cells using proteomic approaches — implications for cellular responses to virus infection. Mol. Cell. Proteomics 4, 902–913.

Laurent-Matha, V., Derocq, D., Prebois, C., Katunuma, N., Liaudet-Coopman, E., 2006. Processing of human cathepsin D is independent of its catalytic function and auto-activation: involvement of cathepsins L and B. J. Biochem. 139, 363–371.
Leong, W.F., Chow, V.T.K., 2006. Transcriptomic and proteomic analyses of rhabdomyosarcoma cells reveal differential cellular gene expression in response to enterovirus 71 infection. Cell. Microbiol. 8, 565–580.
Levy, A.M., Davidson, I., Burgess, S.C., Dan Heller, E., 2003. Major histocompatibility complex class I is downregulated in Marek's disease virus infected chicken embryo fibroblasts and corrected by chicken interferon. Comp. Immunol. Microbiol. Infect. Dis. 26, 189–198.
Li, X.H., Jarosinski, K.W., Schat, K.A., 2006. Expression of Marek's disease virus phosphorylated polypeptide pp38 produces splice variants and enhances metabolic activity. Vet. Microbiol. 117, 154–168.
Lindner, H.A., 2007. Deubiquitination in virus infection. Virology 362, 245–256.
Liu, H.C., Cheng, H.H., Tirunagaru, V., Sofer, L., Burnside, J., 2001. A strategy to identify positional candidate genes conferring Marek's disease resistance by integrating DNA microarrays and genetic mapping. Anim. Genet. 32, 351–359.
Liu, H.C.S., Soderblom, E.J., Goshe, M.B., 2006. A mass spectrometry-based proteomic approach to study Marek's disease virus gene expression. J. Virol. Methods 135, 66–75.
Liu, N., Song, W.J., Wang, P., Lee, K.C., Chan, W., Chen, H.L., et al., 2008. Proteomics analysis of differential expression of cellular proteins in response to avian H9N2 virus infection in human cells. Proteomics 8, 1851–1858.
MacCoss, M.J., Wu, C.C., Yates, J.R., 2002. Probability based validation of protein identifications using a modified SEQUEST algorithm. Anal. Chem. 74, 5593–5599.
Manceau, V., Gavet, O., Curmi, P., Sobel, A., 1999. Stathmin interaction with HSC70 family proteins. Electrophoresis 20, 409–417.
McCarthy, F.M., Bridges, S.M., W.N., Magee, G.B., Williams, W.P., Luthe, D.S., Burgess, S.C., 2006. AgBase: a unified resource for functional genomics analysis in agriculture. Nucleic Acids Res. D599–603.
Morgan, R.W., Sofer, L., Anderson, A.S., Bernberg, E.L., Cui, J., Burnside, J., 2001. Induction of host gene expression following infection of chicken embryo fibroblasts with oncogenic Marek's disease virus. J. Virol. 75, 533–539.
Morimura, T., Hattori, M., Ohashi, K., Sugimoto, C., Onuma, M., 1995. Immunomodulation of peripheral T-cells in chickens infected with Marek's disease virus — involvement in immunosuppression. J. Gen. Virol. 76, 2979–2985.
Morimura, T., Ohashi, K., Kon, Y., Hattori, M., Sugimoto, C., Onuma, M., 1996. Apoptosis and CD8-down-regulation in the thymus of chickens infected with Marek's disease virus — brief report. Arch. Virol. 141, 2243–2249.
Munger, J., Bajad, S.U., Coller, H.A., Shenk, T., Rabinowitz, J.D., 2006. Dynamics of the cellular metabolome during human cytomegalovirus infection. PLoS pathog. 2, 1165–1175.
Nanduri, B., Lawrence, M.L., Vanguri, S., Burgess, S.C., 2005. Proteomic analysis using an unfinished bacterial genome: the effects of subminimum inhibitory concentrations of antibodies on *Mannheimia haemolytica* virulence factor expression. Proteomics 5, 4852–4863.
Nesvizhskii, A.I., Keller, A., Kolker, E., Aebersold, R., 2003. A statistical model for identifying proteins by tandem mass spectrometry. Anal. Chem. 75, 4646–4658.
Niikura, M., Kim, T., Hunt, H.D., Burnside, J., Morgan, R.W., Dodgson, J.B., et al., 2007. Marek's disease virus up-regulates major histocompatibility complex class II cell surface expression in infected cells. Virology 359, 212–219.
Piersanti, S., Martina, Y., Cherubini, G., Avitabile, D., Saggio, I., 2004. Use of DNA microarrays to monitor host response to virus and virus-derived gene therapy vectors. Am. J. Pharmacogenomics 4, 345–356.
Ramaroson, M.F., Ruby, J., Goshe, M.B., Liu, H.C., 2008. Changes in the *Gallus gallus* proteome induced by Marek's disease virus. J. Proteome Res. 7, 4346–4358.
Saldanha, R.G., Xu, N., Molloy, M.P., Veal, D.A., Baker, M.S., 2008. Differential proteome expression associated with urokinase plasminogen activator receptor (uPAR) suppression in malignant epithelial cancer. J. Proteome Res. 7, 4792–4806.
Sarson, A.J., Abdul-Careem, M.F., Zhou, H., Sharif, S., 2006. Transcriptional analysis of host responses to Marek's disease viral infection. Viral Immunol. 19, 747–758.
Schat, K.A., Calnek, B.W., Fabricant, J., 1982. Characterization of 2 highly oncogenic strains of Marek's disease virus. Avian Pathol. 11, 593–605.
Schumacher, D., Tischer, B.K., Trapp, S., Osterrieder, N., 2005. The protein encoded by the U_S3 orthologue of Marek's disease virus is required for efficient de-envelopment of perinuclear virions and involved in actin stress fiber breakdown. J. Virol. 79, 3987–3997.
Shack, L.A., Buza, J.J., Burgess, S.C., 2008. The neoplastically transformed ($CD30^{hi}$) Marek's disease lymphoma cell phenotype most closely resembles T-regulatory cells. Cancer Immunol. Immunother. 57, 1253–1262.
Shevchenko, A., Wilm, M., Vorm, O., Mann, M., 1996. Mass spectrometric sequencing of proteins from silver-stained polyacrylamide gels. Anal. Chem. 68, 850–858.
St Hill, C.A., Sharma, J.M., 1999. Response of embryonic chicken lymphocytes to in ovo exposure to lymphotropic viruses. Am. J. Vet. Res. 60, 937–941.
Thompson, S.R., Sarnow, P., 2000. Regulation of host cell translation by viruses and effects on cell function. Curr. Opin. Microbiol. 3, 366–370.
Wing, S.S., 2003. Deubiquitinating enzymes—the importance of driving in reverse along the ubiquitin–proteasome pathway. Int. J. Biochem. Cell Biol. 35, 590–605.
Witter, R.L., 1997. Increased virulence of Marek's disease virus field isolates. Avian Dis. 41, 149–163.
Xing, Z., Schat, K.A., 2000. Expression of cytokine genes in Marek's disease virus-infected chickens and chicken embryo fibroblast cultures. Immunology 100, 70–76.
Zelivianski, S., Liang, D., Chen, M., Mirkin, B.L., Zhao, R.Y., 2006. Suppressive effect of elongation factor 2 on apoptosis induced by HIV-1 viral protein R. Apoptosis 11, 377–388.
Zhang, C.G., Chromy, B.A., McCutchen-Maloney, S.L., 2005. Host–pathogen interactions: a proteomic view. Expert Rev. Proteomics 2, 187–202.
Zheng, X.J., Hong, L.L., Shi, L.X., Guo, J.Q., Sun, Z., Zhou, J.Y., 2008. Proteomics analysis of host cells infected with infectious bursal disease virus. Mol. Cell. Proteomics 7, 612–625.